2024 International Applied Computational Electromagnetics Society Symposium (ACES-China) | 979-8-3503-5558-1/24/$31.00 ©2024 IEEE | DOI: 10.1109/ACES-China62474.2024.10700004

Hybrid Eccentric SIM With Embedded Ring/Separate Elliptic SEM

Zhen Guan, Feng Han
School of Computing and Information Technology
Great Bay University
Guangdong, China
xmuzg@foxmail.com, feng.han@gbu.edu.cn

Jiawen Li
School of Electronic and Information Engineering
Guangxi Normal University
Guangxi, China
jiawenli@mailbox.gxnu.edu.cn

***Abstract*—In this paper, we propose a complicated biaxially anisotropic multiple spectral integral method (SIM), both nested vertical multilayers and separate eccentric elliptical cylinders embedded in the same lateral layer are considered simultaneously. Furthermore, a hybrid SIM/spectral element method (SEM) is proposed, in which SIM is used as the truncated boundary condition for the discretized arbitrary anisotropic subregions by SEM. Two examples corresponding to these two methods are well matched with COMSOL respectively.**

Keywords*—*SIM; multilayers; eccentric; hybrid SIM/SEM

I. Introduction

The calculation of electromagnetic (EM) scattering is of great research merit in the application of radar detection and antenna propagation [1], which can be roughly divided into two categories.

One is integral method, such as method of moments (MoM) belonging to large-scale spatial Green's function, boundary integral method (BIM) referred to the principle of surface equivalence, and spectral integral method (SIM), which is relevant to the fast Fourier transform (FFT) [2]. The other one is differential method, such as finite element method (FEM) to approximate the function expansion of local domain for finite elements, spectral element method (SEM) concerned to global orthogonal basis functions for each element [3].

Furthermore, hybrid methods that combine the superiority of both types of methods, such as BIM/SEM [4] and FEM/SIM [5], have been developed in recent years. In this work, we propose a complicated SIM to simultaneously calculate the eccentric ellipses of the same region layer and the nested non-concentric ellipses of different region layers. Moreover, SEM for local embedded arbitrary anisotropic ring/separate elliptic regions is considered.

II. Formulation

A. Multi-Layer Eccentric SIM

We first build SIM of the multilayered eccentric elliptical cylinder. In order to construct SIM with multiple nested vertical layers and separate ellipses in the same lateral layer, as shown in Fig. 1, we divide the number of ellipses into two categories.

I. Vertical numbering: the nested radial stratified cylinders are $l_m (1 \le m \le M)$ from the outside to inside, and the regions are $\Omega_{l_m} (1 \le m \le M+1)$.

II. Lateral numbering: the separate eccentric elliptic cylinders $S_n (1 \le n \le N)$ are embedded in the same region Ω_{l_m} enclosed by l_{m-1} and l_m, the corresponding regions are $\Omega_{S_n} (1 \le n \le N)$.

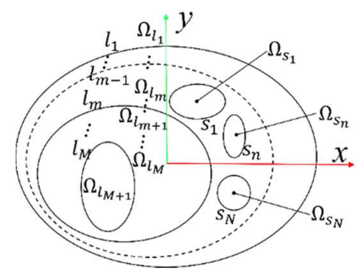

Fig. 1. Multilayered eccentric elliptical magnetodielectric cylinders. (with *$l_M + S_N$ boundary layers and $l_M + S_N + 1$ regions in total*)

For part I, l_m has radiation effects only between the nested adjacent layers l_{m-1}, l_{m+1}, so similar to formula (6) in our previous work [6], the EM radiation matrix can be concisely written as

$$\boldsymbol{Z}^{11} = \begin{bmatrix} \boldsymbol{z}_{J,m,m-1} & \boldsymbol{z}_{M,m,m-1} & \boldsymbol{Z}^{ex}_{J,m,m} & \boldsymbol{Z}^{ex}_{M,m,m} & & \\ & & \boldsymbol{Z}^{in}_{J,m,m} & \boldsymbol{Z}^{in}_{M,m,m} & \boldsymbol{z}_{J,m,m+1} & \boldsymbol{z}_{M,m,m+1} \end{bmatrix} \quad (1)$$

where $\boldsymbol{z}_{K,p,q}$ is the Fourier expansion of Green's function by the surface current density K with the equivalent source point on the qth layer and field point on the pth layer. The superscripts "ex" and "in" represent the exterior and the interior scattering effect generated on the same boundary layer l_m.

For part II, S_n has mutual radiation effects with all $S_n (1 \le n \le N)$, then

$$\boldsymbol{Z}^{22} = \begin{bmatrix} \boldsymbol{z}_{J,n,\alpha} & \boldsymbol{z}_{M,n,\alpha} & \boldsymbol{Z}^{ex}_{J,n,n} & \boldsymbol{Z}^{ex}_{M,n,n} & \boldsymbol{z}_{J,n,\beta} & \boldsymbol{z}_{M,n,\beta} \\ & & \boldsymbol{Z}^{in}_{J,n,n} & \boldsymbol{Z}^{in}_{M,n,n} & & \end{bmatrix} \quad (2)$$

where $1 \le \alpha < n, n < \beta \le N$. Note these separate ellipses can be further developed into vertical multilayered nested ellipses, simply by replacing the formula (3) in (2) with (1).

$$\begin{bmatrix} \boldsymbol{Z}^{ex}_{J,n,n} & \boldsymbol{Z}^{ex}_{M,n,n} \\ \boldsymbol{Z}^{in}_{J,n,n} & \boldsymbol{Z}^{in}_{M,n,n} \end{bmatrix} \quad (3)$$

For commutation on part I and II, since these S_n are located inside the elliptic ring region Ω_{l_m} enclosed by l_{m-1} and l_m. Then the coefficient matrix of l_{m-1}, l_m affected by S_n is $\boldsymbol{Z}^{12}$, the opposite matrix is $\boldsymbol{Z}^{21}$.

$$\boldsymbol{Z}^{12}=\begin{bmatrix} \boldsymbol{z}_{J,m-1,\alpha} & \boldsymbol{z}_{M,m-1,\alpha} & \boldsymbol{z}_{J,m-1,n} & \boldsymbol{z}_{M,m-1,n} & \boldsymbol{z}_{J,m-1,\beta} & \boldsymbol{z}_{M,m-1,\beta} \\ \boldsymbol{z}_{J,m,\alpha} & \boldsymbol{z}_{M,m,\alpha} & \boldsymbol{z}_{J,m,n} & \boldsymbol{z}_{M,m,n} & \boldsymbol{z}_{J,m,\beta} & \boldsymbol{z}_{M,m,\beta} \end{bmatrix} \quad (4)$$

$$\boldsymbol{Z}^{21}=\begin{bmatrix} \boldsymbol{0} & \boldsymbol{z}_{J,n,m-1} & \boldsymbol{z}_{M,n,m-1} & \boldsymbol{z}_{J,n,m} & \boldsymbol{z}_{M,n,m} & \boldsymbol{0} \end{bmatrix} \quad (5)$$

where $\boldsymbol{Z}^{12}$ has non-zero values only in the row where l_{m-1} and l_m reside. Consequently, the compositive matrix system is $\boldsymbol{ZI}=\boldsymbol{V}$, where $\boldsymbol{V}$ is the EM excitation source and

$$\boldsymbol{Z}=\begin{bmatrix} \boldsymbol{Z}^{11} & \boldsymbol{Z}^{12} \\ \boldsymbol{Z}^{21} & \boldsymbol{Z}^{22} \end{bmatrix} \quad (6)$$

$$\boldsymbol{I}=[\boldsymbol{H}_{z,m-1} \quad \overline{\boldsymbol{E}}_{t,m-1} \quad \boldsymbol{H}_{z,m} \quad \overline{\boldsymbol{E}}_{t,m} \quad \boldsymbol{H}_{z,m+1} \quad \overline{\boldsymbol{E}}_{t,m+1}$$
$$\boldsymbol{H}_{z,\alpha} \quad \overline{\boldsymbol{E}}_{t,\alpha} \quad \boldsymbol{H}_{z,n} \quad \overline{\boldsymbol{E}}_{t,n} \quad \boldsymbol{H}_{z,\beta} \quad \overline{\boldsymbol{E}}_{t,\beta}]^{\mathsf{T}} \quad (7)$$

B. Hybrid SIM With Ring/Separate Elliptic SEM

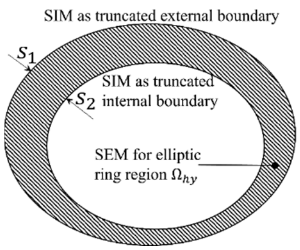

Fig. 2. The ring region by hybrid method with SEM embedded in SIM.

Supposing the media in a certain region is inhomogeneous, which means pure SIM is not available. Then SEM can be used to solve the interior region problem, while SIM is used as the truncated boundary condition. As shown in Fig. 2, since the interior of the ring region Ω_{hy} needs to be discretized, the computing nodes are not only on the boundaries S_1, S_2, but also inside Ω_{hy}, then the coupled matrix is

$$\boldsymbol{Z}_{\mathrm{hy}}^{ring}=\begin{bmatrix} \boldsymbol{Z}_{J,1,1}^{ex} & \boldsymbol{Z}_{M,1,1}^{ex} & \boldsymbol{0} & & \\ \boldsymbol{Z}^{b_1b_1}\boldsymbol{T}_1 & \boldsymbol{Z}_{S_1}\boldsymbol{T}_1 & \boldsymbol{Z}^{b_1i} & & \\ \boldsymbol{Z}^{ib_1}\boldsymbol{T}_1 & & \boldsymbol{Z}^{ii} & \boldsymbol{Z}^{ib_2}\boldsymbol{T}_2 & \\ & & \boldsymbol{Z}^{b_2i} & \boldsymbol{Z}^{b_2b_2}\boldsymbol{T}_2 & \boldsymbol{Z}_{S_2}\boldsymbol{T}_2 \\ & & & \boldsymbol{Z}_{J,2,2}^{in} & \boldsymbol{Z}_{M,2,2}^{in} \end{bmatrix} \quad (8)$$

where the superscripts b_1, b_2 means on the boundary S_1 and S_2 respectively, and i means inside the region Ω_{hy}. The variables corresponding to (8) are

$$\boldsymbol{I}_{\mathrm{hy}}^{ring}=[\boldsymbol{H}_{z,1} \quad \overline{\boldsymbol{E}}_{t,1} \quad \boldsymbol{H}^{i} \quad \boldsymbol{H}_{z,2} \quad \overline{\boldsymbol{E}}_{t,2}]^{\mathsf{T}} \quad (9)$$

For the hybrid SIM/SEM solution, $\boldsymbol{Z}_{ring}^{\mathrm{hy}}$ is inserted as a part into $\boldsymbol{Z}^{11}$ in (1) or into $\boldsymbol{Z}^{22}$ in (2) if $\boldsymbol{Z}^{22}$ has nested layers.

In particular, when $S_2 \to 0$, then the ring region will be infinitely approximated to an elliptic region. $\boldsymbol{Z}_{\mathrm{hy}}^{ellipse}$ derived from the first three rows and first three columns of $\boldsymbol{Z}_{\mathrm{hy}}^{ring}$ can replace (3) in $\boldsymbol{Z}^{22}$ or that matrix for the last elliptic region $\Omega_{l_{M+1}}$ in $\boldsymbol{Z}^{11}$.

III. Numerical Results

In this section, we present two numerical examples to verify the expected efficiency of the proposed eccentric SIM and hybrid SIM/SEM by comparing its computation results with the commercial software COMSOL.

A. 3-Layer Eccentric SIM

As shown in Fig. 3, the 3-layer biaxially anisotropic medium eccentric elliptical cylinders are excited by the source which are three unit magnetic dipole transmitters, and the 49 receivers are a circular array around the object cylinders, all corresponding parameters are shown in Table I and Table II, the unit of length on the coordinate is m.

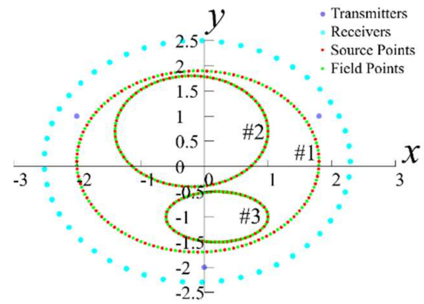

Fig. 3. The 3-layer eccentric elliptical magnetodielectric anisotropic cylinders.

TABLE I. Model Parameters of Each Ellipse

Parameters / Ellipse	Position and size		Medium of surrounded region		
	Center coordinate	*Axis length*	(ϵ_x, ϵ_y)	(σ_x, σ_y)	μ
#1	(-0.1, 0.1)	(1.9, 1.8)	(1.0, 1.0)	(0.0000,0.0000)	1.0
#2	(-0.2, 0.7)	(1.2, 1.1)	(1.5, 1.4)	(0.0001,0.0002)	1.1
#3	(0.2, -1.0)	(0.8, 0.5)	(2.0, 1.8)	(0.0002,0.0003)	1.2

TABLE II. Parameters of Transmitters and Receivers

Transmitters	***Number***	***Center coordinate***		
	3	(1.8, 1.0)	(-2.0, 1.0)	(0.0, -2.0)
Circular array of receivers	***Number***	***Center coordinate***		***Radius***
	49	(-0.11, 0.10)		2.4

The accuracy of EM field values along the three boundaries of the elliptical cylinders will be verified by COMSOL. As shown in Fig. 4, SIM can achieve 1% error by using only 200 sampling points on three layers, that is, with spatial sampling densities (SD) as 5 PPW, compared with COMSOL using 392452 triangular elements and 196679 sampling points, that is, SD = 35 PPW. The errors of the real and imaginary parts of the tangential fields $\boldsymbol{E}_t$ are 0.0086 and 0.0109 respectively, and the corresponding errors of $\boldsymbol{H}_z$ are 0.0033 and 0.0021 respectively. In this case, SIM only uses 0.79 s time and 1881.0 MB memory, while COMSOL requires 22 s time and 6570.9 MB memory.

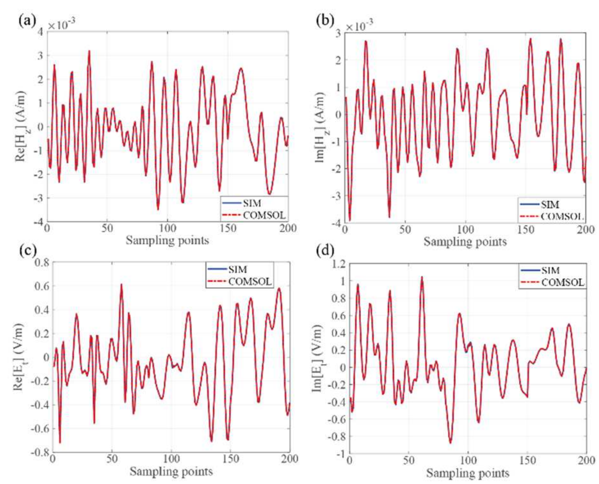

Fig. 4. Comparisons of the total EM fields along three elliptical boundaries computed by SIM and COMSOL.

B. 6-Layer Hybrid SIM/SEM

In this case, as shown in Fig. 5, we retain the parameters of the three ellipses of case *A*, whereas for the sake of exploration of incorporating SEM into SIM, we set the medium parameters $\bar{\bar{\boldsymbol{\epsilon}}}_{\boldsymbol{t}}, \bar{\bar{\boldsymbol{\sigma}}}_{\boldsymbol{t}}, \boldsymbol{\mu}$ for the third ellipse of case *A* (#6 in this case) to $\begin{pmatrix}1.5 & 0.2\\ 0.3 & 2.0\end{pmatrix}, \begin{pmatrix}0.0001 & 0.0002\\ 0.0003 & 0.0004\end{pmatrix}, 1.5$ respectively, and this separate elliptic region is discretized by SEM. At the same time, we also added #3 with radius 1.0 m and the same center coordinate as #2, which surrounds a ring region with the same parameters as #6, and is also discretized by SEM, as shown in Fig. 6. The corresponding parameters for added nested #4 and #5 are (3.0, 2.6), (0.0004, 0.0005), 1.4 and (3.5, 3.0), (0.0005, 0.0004), 1.5 respectively. Their center coordinates are (-0.1, 0.6) and (0.0, 0.3), axis lengths are (0.7, 0.8), (0.4, 0.3).

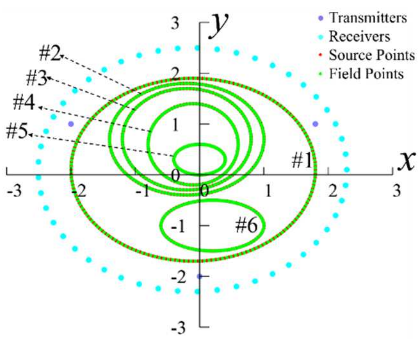

Fig. 5. The 6-layer eccentric elliptical magnetodielectric anisotropic cylinders.

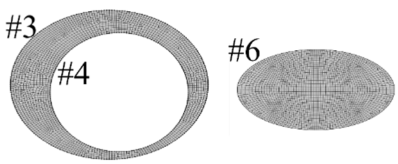

Fig. 6. Inhomogeneous subregions discretized by SEM in Fig. 5.

Fig. 7(a)–(f) shows the relative errors of the scattered fields at the receiver array, in which SIM/SEM only uses 4485 quadrilateral elements and 5494 sampling points, and the SD is 23 PPW only in the regions enclosed by #3 and #6, the SD of other regions is as low as that of case *A*. While COMSOL needs to discrete the entire calculation regions, with 388874 triangular elements and 194890 sampling points. The minimum SD of the whole area is 27 PPW. Then the relative errors of $\boldsymbol{E}_x^{sct}, \boldsymbol{E}_y^{sct}, \boldsymbol{H}_z^{sct}$ are 0.0092, 0.0106 and 0.0100, respectively. As can be seen, the hybrid SIM/SEM calculations reach good matches with the results implemented by COMSOL.

IV. Conclusion

In this work, we propose a complicated multilayered eccentric SIM that simultaneously considers both nested vertical layers and separate elliptical cylinders embedded in the same lateral layer. The effects of EM radiation between these ellipses are related to the convolution integral of Green's functions in matrix systems. The hybrid SIM with ring/separate elliptic SEM is also proposed, in which several inhomogeneous subregions of the model are calculated by SEM. Two numerical cases are implemented not only to validate the EM fields along boundaries but also to validate the scattered EM fields at the receiver array. Both of the proposed methods can achieve 1% error and are superior to COMSOL in terms of efficiency.

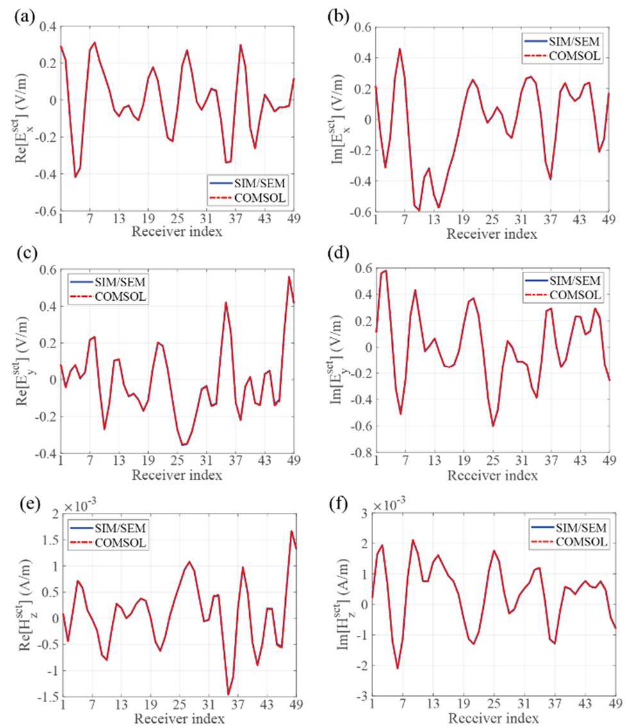

Fig. 7. Comparisons of the scattered EM fields at the receiver array computed by hybrid SIM/SEM and COMSOL.

References

[1] S. Karan and V. B. Erturk, "Analysis of input impedance and mutual coupling of microstrip antennas on multilayered circular cylinders using closed-form green's function representations," IEEE Trans. Antennas Propag., 62(11), pp. 5485–5496, Nov. 2014.

[2] Z. Guan, Y. Zhang, F. Han, C. Zhu, and Q. H. Liu, "Fast exponentially convergent solution of electromagnetic scattering from multilayer concentric magnetodielectric cylinders by the spectral integral method," IEEE Trans. Microw. Theory Tech., 68(6), pp. 2183–2193, Jun. 2020.

[3] C. Pozrikidis, "Introduction to Finite And Spectral Element Methods Using MATLAB," New York: Chapman and Hall Press, 2014.

[4] J. Niu, M. Luo, Y. Fang, and Q. H. Liu, "Boundary integral spectral element method analyses of extreme ultraviolet multilayer defects," J. Opt. Soc. Amer. A, Opt. Image Sci., 31(10), pp. 2203–2209, Oct. 2014.

[5] Z. Sun, M. Zhuang, and Q. H. Liu, "A 3D finite element spectral integral (FESI) method for acoustics," Appl. Math. Model., 127(2024), pp. 696-710, Mar. 2024.

[6] Z. Guan, J. Li, and F. Han, "Exponential accuracy solutions of 2-D electromagnetic scattering from multilayered nonconcentric elliptical magnetodielectric cylinders under TE illumination," IEEE Trans. Microw. Theory Tech., 72(5), pp. 2914-2926, May 2024.